Chemical Engineering Journal 431 (2022) 133282

Contents lists available at ScienceDirect

Chemical Engineering Journal

journal homepage: www.elsevier.com/locate/cej

Pyrazole bridges ensure highly stable and insensitive bistetrazoles

Jatinder Singh [a], Richard J. Staples [b], Joseph P. Hooper [c], Jean'ne M. Shreeve [a,*]

[a] Department of Chemistry, University of Idaho, Moscow, ID 83844-2343, United States
[b] Department of Chemistry, Michigan State University, East Lansing, MI 48824, United States
[c] Department of Physics, Naval Postgraduate School, Monterey, CA 93943, United States

A B S T R A C T

In the quest for efficient and thermally stable insensitive materials, the inclusion of a bridging molecule between symmetric or asymmetric azole units has recently emerged as a fruitful approach. However, the synthesis of new compounds with high density in combination with high thermal stability and insensitivity often occurs only with difficulty. Now a new class of pyrazole-bridged bistetrazole and bis(1-hydroxytetrazolyl) compounds was synthesized and fully characterized by NMR, IR spectroscopy, and elemental analysis. Thermal behavior was investigated by using differential scanning calorimetry (DSC), and thermal gravimetric analysis (TGA). The solid-state structures of the diammonium salt (**9**) based on 4-nitro-1*H*-pyrazole, and 5,5′-(4-chloro-1*H*-pyrazole-3,5-diyl)bis(1*H*-tetrazole) (**18**) were determined by single-crystal X-ray diffraction. These pyrazole-bridged bistetrazole compounds exhibit excellent thermal stabilities with high decomposition temperatures, moderate heats of formation, high nitrogen content, and insensitivities to impact and friction. Additionally, introduction of a halogen atom at the 4-position of the pyrazole ring gives rise to a new active heterocycle which holds considerable promise as a suitable substrate for further transformation.

1. Introduction

Growing demand for thermally stable insensitive materials, in tandem with increasing initiatives to shed dependence on carbon-based compounds, has motivated the study of nitrogen-rich high-density materials.[1] Our aim is to develop safe and eco-friendly compounds with high decomposition temperatures, moderate heats of formation, and low sensitivities.[2] This can be realized via the syntheses of azole-containing compounds with N═N, N—N, C═N, and C—N bonds in order to attain quality heats of formation, and increasing hydrogen-bond networks through the introduction of nitro ($-NO_2$), nitroamino ($-NHNO_2$), azido (N_3), or N-oxide (N → O) groups which lead to high density.[3] Among the nitrogen-rich azoles, the tetrazole moiety continues to attract considerable research attention owing to good heats of formation arising from the presence of many nitrogen-nitrogen bonds and its high level of environmental compatibility.[4] The quest for new tetrazole-containing compounds has been an integral part of such research, which, in turn, has resulted in many tetrazole combined frameworks with density increasing functional groups. Some of these compounds have been successfully applied in a multitude of roles such as gas generators in automobile airbags (Fig. 1).[5] However, compounds which contain the tetrazole ring with such functional groups are often sensitive to external stimuli and exhibit low decomposition temperatures, which limit their practical applications.[6] Therefore, it is of significant fundamental and applied interest to synthesize tetrazole compounds that are thermally stable, insensitive to friction, impact, and sparks, and that can meet requirements for both military and civilian purposes.[7].

Enormous progress in the synthesis of such materials has led to the emergence of strategies to tailor their properties.[8] A complementary approach to achieve good thermal stability and low sensitivity requires the inclusion of a bridging molecule between symmetrical or asymmetric azole units.[9] Bridging moieties such as -N = N-, -NH-, -C(O)- and -C–C- have been extensively used to connect two or more energetic rings.[10] Recently, azole bridges such as 1,2,4-oxadiazole, and 1,3,4-oxadiazole have attracted considerable research attention as being newly important to synthesize thermostable and insensitive materials.[11,12] To this end, realization of new azole-bridged compounds with easy functionalization, up scalable procedures and improved thermostability is essential to satisfy safety requirements and practical applications.

Pyrazoles are five-membered aromatic heterocycles that constitute a class of compounds particularly valuable in organic transformations.[13] Substituted pyrazoles have found application in a plethora of cases, ranging from agriculture and technology to exploiting a full spectrum of biological activities.[14] They have also been investigated owing to their high thermal stabilities. The use of the pyrazole ring in the synthesis of new materials not only improves the thermal stability but also provides opportunities for easy functionalization at the three-carbon centers, making the new heterocycle a more useful and suitable

* Corresponding author.
E-mail address: jshreeve@uidaho.edu (J.M. Shreeve).

https://doi.org/10.1016/j.cej.2021.133282
Received 28 July 2021; Received in revised form 13 October 2021; Accepted 27 October 2021
Available online 3 November 2021

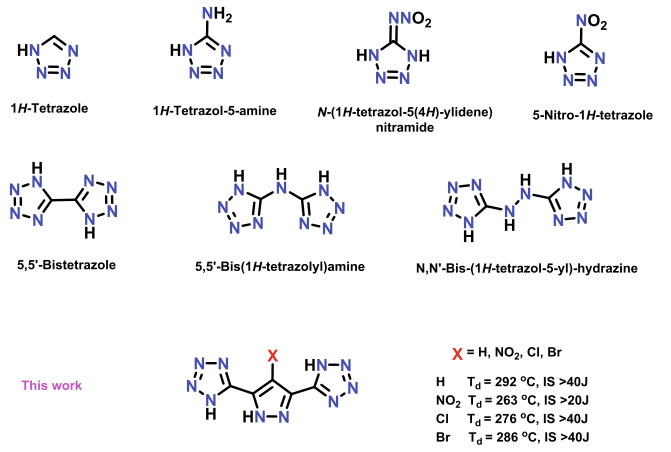

Fig. 1. Examples of various types of mono and bistetrazole compounds.

substrate for further transformations.[15] Now we have synthesized substituted pyrazole-bridged bistetrazole derivatives including 5,5′-(1*H*-pyrazole-3,5-diyl)bis(1*H*-tetrazole), **3**, and 5,5′-(4-nitro-1*H*-pyrazole-3,5-diyl)bis(1*H*-tetrazole), **4**, using 1*H*-pyrazole-3,5-dicarbonitrile, **1**, and 4-nitro-1*H*-pyrazole-3,5-dicarbonitrile, **2**, as precursors. Mild halogenation of 5,5′-(1*H*-pyrazole-3,5-diyl)bis(1*H*-tetrazole), **3**, at the 4-position was carried out using Oxone® (potassium peroxymonosulfate) with halide salts. The resulting halo-nitrogen-rich compounds were found to be highly stable with good density, lower sensitivity, and good heats of formation. In addition, the oxidation of compound **3** with Oxone® gave the pyrazole-bridged bis(1-hydroxytetrazolyl) derivative **20**. Compound **20** and its salts (**21**, **22**) also exhibit good density high thermal stability and lower sensitivity.

2. Results and discussion

2.1. Synthesis

The reaction of 1*H*-pyrazole-3,5-dicarbonitrile (**1**) with sodium azide in the presence of zinc chloride resulted in the formation of the pyrazole-bridged derivative 5,5′-(1*H*-pyrazole-3,5-diyl)bis(1*H*-tetrazole), **3**, as a white solid in 93% yield (Scheme 1). Compound **4** with 4-nitro-1*H*-pyrazole and bis(1*H*-tetrazole) was formed when **2** was reacted with sodium azide in the presence of zinc chloride (Scheme 1).

The 4-position of compound **3** was halogenated using Oxone®/KX (X = Cl, Br, I) (Scheme 2). The chloro and bromo derivatives were obtained selectively and quantitatively, whereas the iodo derivative was obtained as an inseparable mixture with the starting material. The oxidation of compound **3** with Oxone® formed the pyrazole-bridged bis (1-hydroxytetrazolyl) derivative **20**. As is well known, salt formation can improve sensitivity and thermal stability; therefore, **3**, **4**, **13** and **20** were reacted with various nitrogen-rich bases in acetonitrile to give 1:2 salts (Schemes 1 and 2).

2.2. Spectral studies of compounds

New compounds have been fully characterized by NMR [^{1}H, ^{13}C{^{1}H}, and ^{15}N{^{1}H}] and IR spectra as well as elemental analysis. In the ^{13}C{^{1}H} NMR spectra, signals corresponding to the tetrazole carbon atoms in compounds **3–19** were observed over the range of 147.8 to 159.8 ppm. Due to the similar electronic environment at the 3,5-positions in the pyrazole ring, the two carbon signals in compounds **3–19** are averaged to one signal in the range of 131.5 to 140.2 ppm. The carbon at the 4-position of the pyrazole ring was observed at 105.6 ppm in compound **3**, 131.5 ppm in compound **4**, 94.2 ppm in compound **13,** 109.0 ppm in compound **18**, and 61.9 ppm in compound **19.** The bromo and iodo substitution results in the upfield shift of the carbon at the 4-position of the pyrazole ring, whereas the chloro substitution results in the downfield shift. The downfield shift of carbon at the 4-position of the pyrazole ring was observed at 109.1 ppm in compound **20**, 104.9 ppm in compounds **21** and **22.** Upfield shifts of C4-carbon signals were observed concomitantly with salt formation in **5–22**. The ^{15}N NMR spectra of **8**, **12,** and **17** are given in Fig. 2. Signals corresponding to the tetrazole nitrogen atoms attached to the pyrazole moiety are averaged to two signals, 4.06 to 8.53 ppm for anionic nitrogen atoms and −34.58 to −82.92 ppm for the other two nitrogen atoms. Signals of the pyrazole ring nitrogen atoms are in the range −166.29 to −187.94 ppm. The ^{15}N signals corresponding to the nitro group in compounds **2**, **4** and **9–12** are in the range of −15.93 to −24.10 ppm.

2.3. Crystal structure

Crystals suitable for single-crystal X-ray analysis for compounds **9** and **18** were obtained through the slow evaporation of a saturated solution in a methanol/water mixture at room temperature. Crystal structures are given in Figs. 3 and 4. Crystallographic data and data collection parameters, bond lengths, and bond angles are given in the SI. Compound **9**·0.5H_2O crystallizes in the monoclinic space group *C*2/c with a calculated crystal density of 1.675 g cm^{-3} at 100 K. In the crystal structure are two NH_4^+ cations with 0.5 water molecules per molecule dianion. In the crystal packing of **9**·0.5H_2O, there are many strong intermolecular hydrogen bonds between the NH_4 cations and the nitro groups and ring nitrogen atoms of the tetrazole moiety (Fig. 3b). Additionally, the three rings are stacked in a zig-zag fashion, giving rise to π-π interactions. All these interactions which arise from the presence of the cations contribute significantly to the high thermal stability and reduced sensitivity. Compound **18**·H_2O crystallizes in the monoclinic space group $P2_1/c$ with a calculated crystal density of 1.768 g cm^{-3} at 100 K. The compound crystallizes with water molecules in the lattice which gives rise to intermolecular hydrogen bond interactions (Fig. 4).

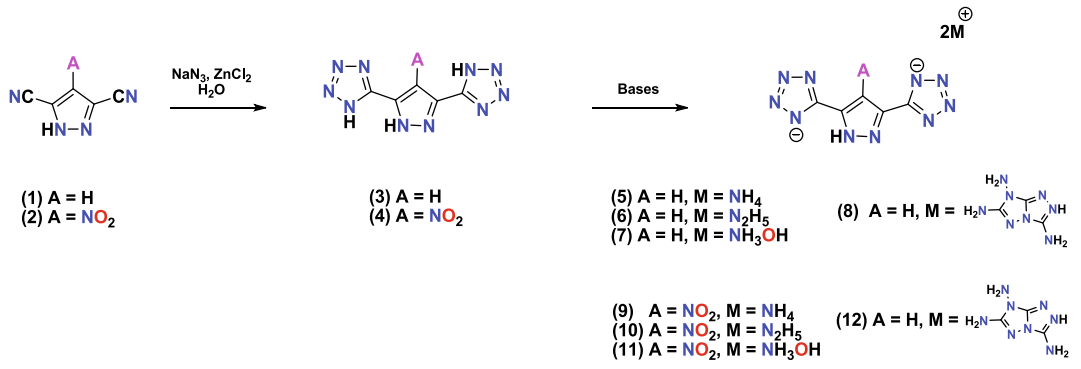

Scheme 1. Synthesis of pyrazole-bridged bistetrazole compounds **3** and **4** and their salts.

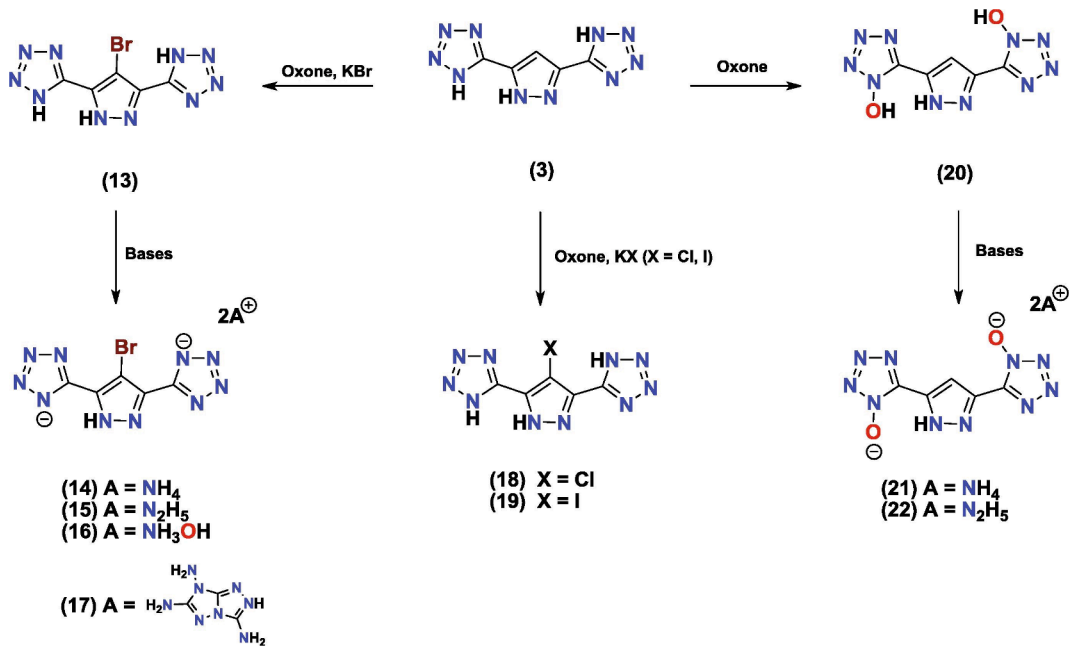

Scheme 2. Halogenation of pyrazole-bridged bistetrazole compound **3;** conversion of **3** to bis(1-hydroxytetrazol-5-yl) derivative **20;** and syntheses of salts **14**–**17** and **21**–**22**.

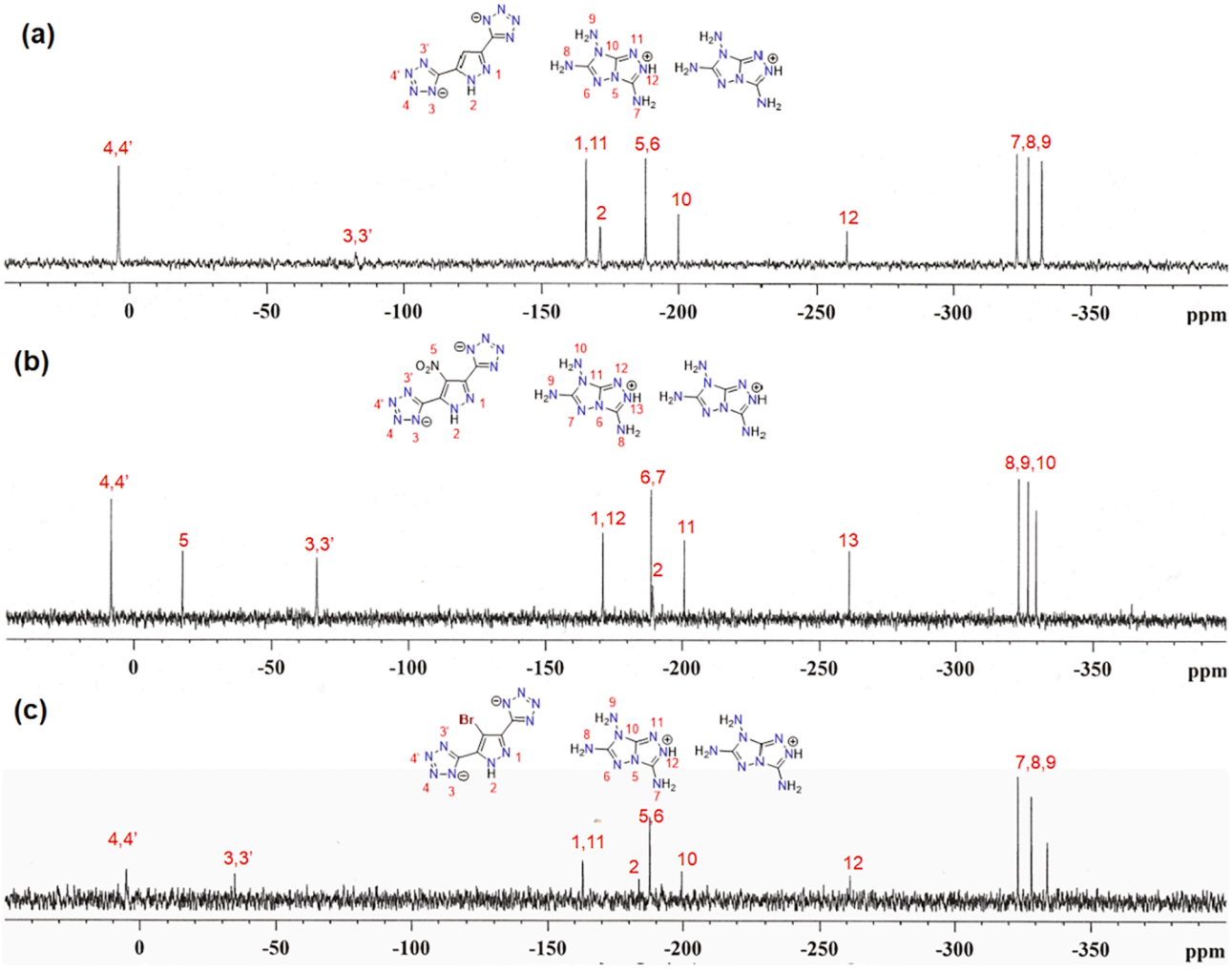

Fig. 2. ^{15}N NMR spectra of (a) 8, (b) 12, and (c) 17.

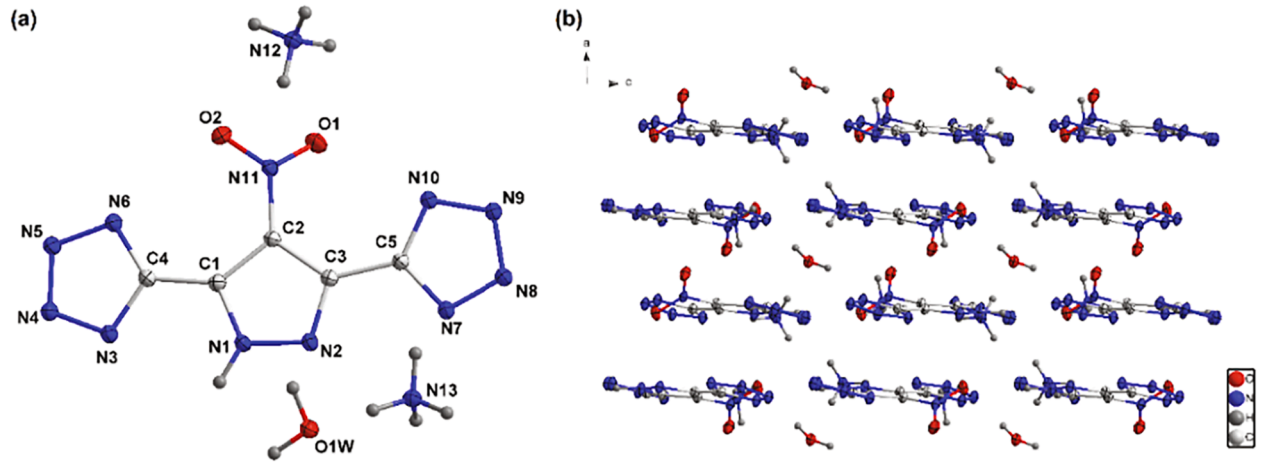

Fig. 3. (a) Thermal ellipsoid plot (50%) and labeling scheme for **9**·0.5H_2O. (b) Ball-and-stick packing diagram of **9**·0.5H_2O .

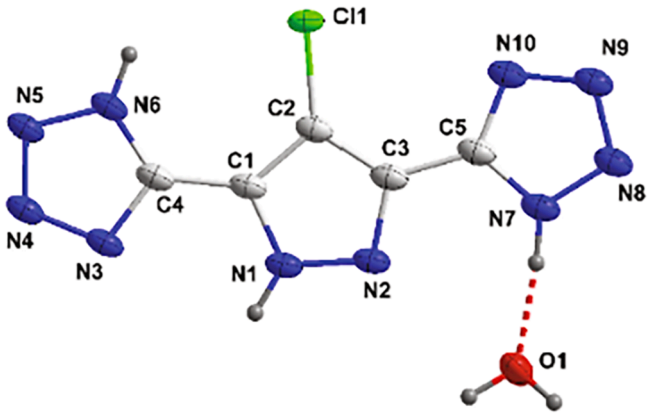

Fig. 4. Thermal ellipsoid plot (50%) and labeling scheme for **18**·H_2O.

2.4. Hirshfeld surface and Non-covalent interactions

Since crystal packing strongly influences the physical properties of compounds, two-dimensional (2D) fingerprints and the associated Hirshfeld surfaces [16,17] were employed by using Crystalexplorer17.5 to understand structure-properties and intermolecular interactions in **9**·0.5H_2O. Red and blue dots on the Hirshfeld surface analysis represent high and low close contacts, respectively. In Fig. 5a–5c, stabilizing interactions such as N···H (51.5%) and O···H (13.8%) are seen in **9**·0.5H_2O, which contribute to the total weak interactions of 65.3%. As shown in Fig. 5c, high percentages (17.8%) of N···N, and N···C interactions were observed which denote π − π stacking for **9**·0.5H_2O. This is also supported by noncovalent interaction (NCI) plots of gradient isosurfaces for **9**·0.5H_2O. The green surface can be clearly seen from the Fig. 5d due to the presence of π-π interactions.[18] The combination of N···H, O···H and π-π interactions leads to the high insensitivity and high molecular stability of compound **9**·0.5H_2O (Fig. 5). The calculated results agree well with the sensitivity data from experiment, which shows impact sensitivity and friction sensitivity of **9**·0.5H_2O is > 40 J and > 360 N, respectively.

2.5. Physicochemical and energetic properties

The thermal stabilities of the new energetic materials **3**–**22** were determined using Differential scanning calorimetry (DSC) at a heating rate of 5 °C min^{-1} (Table 1). The DSC and TGA for compounds **3**, **4**, **13**, and **17** are given in the Supporting Information. The decomposition temperatures for all the compounds occur between 212 (**10**) and 307 (**6**) °C. The densities were measured using a gas pycnometer at 25 °C and the values range between 1.56 (**6**) to 2.06 (**13**) g/cm^3. Compound **3** exhibits a density of 1.61 g cm^{-1} at 298 K. The introduction of an NO_2 group at the C4-position increases the density from 1.61 g cm^{-1} to 1.71 g cm^{-1}. The NO_2 group at the 4-position of pyrazole increases the possibility of inter- and intra- molecular H-bonding, which makes a positive contribution to the density. The densities of compounds **13**–**17** were found to be higher due to the presence of the bromine atom. Compound **13** exhibits density of (2.06 g/cm^3), and its energetic salts have densities range between 1.86 and 1.94 g/cm^3. With the exception of compounds **5** and **6**, all other compounds are more dense than TNT. Compound **20** exhibits higher density (1.71 g cm^{-1} at 298 K) in comparison to compound **3** due to the presence of bis(1-hydroxytetrazol-5-yl) units**.** Energetic salts **21** and **22** also exhibit higher density in comparison to compounds **5** and **6**.

Heats of formation of compounds **3–22** were calculated based on isodesmic reactions using the Gaussian 03 (revision D.01) suite of programs. All the compounds (except **5, 6** and **18**) have relatively high positive heats of formation (ΔH_f) which fall between 496.2 and 2200.3 kJ mol^{-1} and are significantly higher than TNT (−59.4 kJ mol^{-1}), and TATB (−154.2 kJ mol^{-1}) (Table 1). Based on the values of the calculated heats of formation and experimental densities, detonation properties of **3**–**12** and **18**–**22** were determined using EXPLO5 (version 6.01). The detonation properties of **13**–**17** were calculated using the Cheetah 8.0 program. The detonation pressures (*P*) for **3**–**22** range between 9.70 and 26.9 GPa with the detonation velocities (D_v) between 5553 and 8338 m s^{-1}. All compounds, except **3, 13** and **18**, have better detonation properties than TNT, while compounds **10** (*P*: 25.0 GPa, D_v: 8338 m s^{-1}), **11** (*P*: 25.4 GPa, D_v: 8235 m s^{-1}) and **22** (*P*: 24.0 GPa, D_v: 8336 m s^{-1}), exhibit detonation properties approaching TATB (*P*: 31.2 GPa, D_v: 8114 m s^{-1}). Impact and friction sensitivity values were obtained by using a BAM drop hammer apparatus and BAM friction tester, respectively. Except for **4** (IS: 20 J, FS: 240 N) (Table 1), all the compounds were found to be insensitive (IS > 35 J, FS > 360 N) to both impact and friction.

3. Conclusions

Azole-bridged compounds offer powerful synthetic routes to new molecules with tunable properties. Insertion of a pyrazole-bridge between two tetrazole units increases the thermal stability while concomitantly decreasing sensitivity to impact and friction. The densities of the new compounds are in the range 1.56 to 2.06 g/cm^3, which places most of them in a class of relatively dense compounds with good heats of formation. Mild, green halogenation of 5,5′-(1*H*-pyrazole-3,5-diyl)bis(1*H*-tetrazole) at the 4-position was possible using Oxone® and

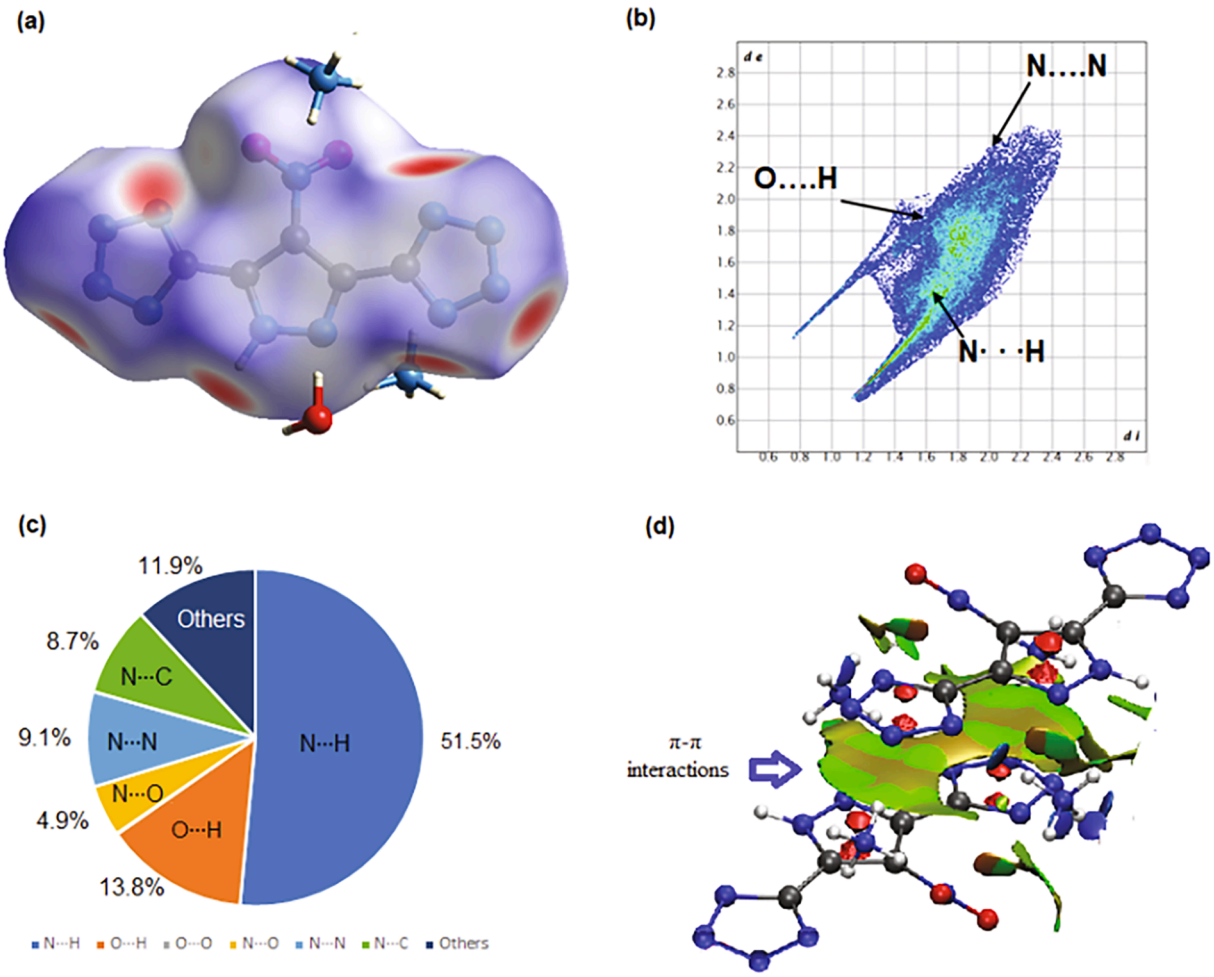

Fig. 5. (a) Hirshfeld surface graph of **9**·0.5H_2O. (b) 2D fingerprint plot of **9**·0.5H_2O. (c) percentage contributions of the individual atomic contacts to the Hirshfeld surface for **9**·0.5H_2O. (d) NCI plots of gradient isosurfaces for **9**·0.5H_2O.

halide salts. This method can be utilized to further functionalize azole rings in a variety of materials. The oxidation of compound **3** with Oxone® gave the pyrazole-bridged bis(1-hydroxytetrazolyl) derivative with good density, thermal stability, and insensitivity**.** Overall, insertion of pyrazole-bridges between tetrazole rings offers a positive route to improve thermal stability and sensitivity with the option of functional substitution to enhance density.

4. Experimental section

Caution! Although no explosions or hazards were observed during the preparation and handling of these compounds, all the compounds investigated are energetic materials. Mechanical actions involving scratching or scraping must be avoided. In addition, all the compounds must be synthesized only on a small scale. All manipulations must be carried out in a hood behind a safety shield. Eye protection and leather gloves must be worn at all times.

4.1. General methods

All reagents were purchased from VWR or AK Scientific in analytical grade and were used as supplied, if not stated otherwise. ^{1}H and ^{13}C NMR spectra were recorded using a 300 MHz (Bruker AVANCE 300) NMR spectrometer operating at 300.13 and 75.48 MHz, respectively. A 500 MHz (Bruker AVANCE 500) NMR spectrometer operating at 50.69 MHz was used to obtain ^{15}N NMR spectra. Chemical shifts in the ^{1}H and ^{13}C NMR spectra are reported relative to Me_4Si and ^{15}N NMR spectra to $MeNO_2$. The melting and decomposition (onset) points were obtained on a differential scanning calorimeter (TA Instruments Company, Model: Q2000) at a scan rate of 5 °C min^{-1}. IR spectra were recorded on a FT-IR spectrometer (Thermo Nicolet AVATAR 370) as thin films using KBr plates. Density was measured at room temperature by employing a Micromeritics AccuPyc II 1340 gas pycnometer. The impact (IS) and friction sensitivities (FS) were measured by employing a standard BAM drop hammer and BAM friction tester. Elemental analyses (C, H, N) were determined using a Vario Micro cube Elementar Analyser.

A yellow block-shaped crystal (**9**·0.5H_2O) with dimensions 0.10 × 0.10 × 0.08 mm^3 and a colorless irregular-shaped- crystal (**18**·H_2O) with dimensions 0.18 × 0.09 × 0.05 mm^3, were mounted on a nylon loop with Paratone oil. Data were collected using a XtaLAB Synergy, Dualflex, HyPix diffractometer equipped with an Oxford Cryosystems low-temperature device, operating at T = 100.00(10) K. The structures were solved by a dual method using the ShelXT [23] structure solution program. The structure was refined by Least Squares using version 2018/2 of XL [24] incorporated in Olex2.[25] All non-hydrogen atoms were refined anisotropically. Hydrogen atom positions were calculated geometrically and refined using the riding model, except for the hydrogen atom on non-carbon atom(s) which were found by difference Fourier methods and refined isotropically when data permits. In structure **18**·H_2O, the value of Z' is 0.5. This means that only half of the formula unit is present in the asymmetric unit, with the other half consisting of symmetry equivalent atoms.

Table 1
Energetic properties of compounds **3**–**22**.

	ρ[a] (g/cm^3)	D_v[b] (m s^{-1})	P[c] (GPa)	ΔH_f[d] (kJmol^{-1})	T_d[e] (°C)	IS[f] (J)	FS[g] (N)	N[h]%
3	1.61	5755	9.70	151.0	293	>40	>360	68.6
4	1.71	6940	16.8	136.2	247	20	240	61.8
5	1.58	7393	17.6	496.2	302	>40	>360	70.5
6	1.56	7939	21.0	850.8	307	>40	>360	73.1
7	1.67	8297	24.6	619.0	285	>40	>360	62.2
8	1.69	7829	21.0	1330.5	248	>40	>360	71.0
9	1.68	7998	22.8	498.2	278	35	>360	64.2
10	1.65	8338	25.0	844.3	212	36	>360	67.0
11	1.66	8235	25.4	640.3	258	39	>360	57.7
12	1.65	7968	22.6	1741.0	260	>40	>360	67.8
13	2.06	6396	17.4	578.1[i]	286	>40	>360	49.5
14	1.94	7524	23.8	996.4[i]	285	>40	>360	53.0
15	1.90	7986	26.9	1309.4[i]	289	>40	>360	56.5
16	1.91	7710	26.5	1108.6[i]	252	>40	>360	48.1
17	1.86	8019	25.3	2200.3[i]	255	>40	>360	61.6
18	1.72	5553	9.98	124.01	276	>40	>360	58.7
20	1.71	7887.5	23.7	800.3	270	>40	>360	59.3
21	1.69	7849.2	20.8	214.1	291	>40	>360	62.2
22	1.65	8335.8	24.0	566.4	296	>40	>360	65.3
TNT[j]	1.65	6824	19.4	−59.4	295	15	>353	18.5
TATB[k]	1.94	8201	28.0	−154.2	360	50	>360	32.5
LLM-116[l]	1.90	8240	32.8	96.3	182	>40	>360	40.4
LLM-105[m]	1.91	8560	33.4	−12.0	342	28	>360	38.9

[a] Density – gas pycnometer at 25 °C.
[b] Calculated detonation velocity.
[c] Calculated detonation pressure.
[d] Calculated molar enthalpy of formation.
[e] Temperature of decomposition (onset).
[f] Impact sensitivity.
[g] Friction sensitivity.
[h] Nitrogen content.
[i] Calculated using Cheetah 8.0 program.
[j] Ref. [19].
[k] Ref. [20].
[l] Ref. [21].
[m] Ref. [22]. All compounds were obtained as anhydrous powders to determine the properties in Table 1.

4.2. Theoretical study

The heats of formation for **3**–**22** and their salts were obtained by using isodesmic reactions (SI). The geometric optimization and frequency analyses of the structures are based on available single crystal structures and using the B3LYP functional with the 6–31 + G** basis set. Single-point energies were calculated at the MP2/6–311++G** level. [26] Atomization energies for cations were obtained by employing the G^2*ab initio* method.[27] All of the optimized structures were characterized to be true local energy minima on the potential energy surface without imaginary frequencies. For energetic salts, the solid-phase heats of formation were calculated based on the Born–Haber energy cycle. [28] All calculated gas-phase enthalpies for covalent materials are converted to solid phase values by subtracting the empirical heat of sublimation obtained based on Trouton's rule.[29]

4.2.1. Synthesis of 1H-pyrazole-3,5-dicarbonitrile (1)

To a mixture of 1*H*-pyrazole-3,5-dicarboxamide (3.72 g, 24.00 mmol) in acetonitrile (70 mL) at 0 °C was added $POCl_3$ (11.25, mL, 120 mmol). The mixture was stirred with heating in a sealed stainless-steel tube at 120 °C for 12 h. It was poured into water/ice and extracted with CH_2Cl_2 (3 × 50 mL). The organic layer was dried over Na_2SO_4, filtered, and evaporated to give **1** as a white solid. Yield: 71%; T_m (onset) = 194 °C; ^{1}H NMR (300 MHz, d_6-DMSO): 7.84 (s, 1H); ^{13}C NMR (75 MHz, d_6-DMSO): 119.9, 118.6, 111.4; IR (ν, cm^{-1}): 3248, 3147, 2258, 1537, 1410, 1269, 1201, 1134, 1024, 993, 837, 776, 679, 659. Elemental analysis: Calcd (%) for $C_5H_2N_4$ (118.10): C, 50.85; H, 1.71; N, 47.44; Found: C 51.14, H 2.10, N 46.59.

4.2.2. Synthesis of 4-nitro-1H-pyrazole-3,5-dicarbonitrile (2)

To a mixture of 4-nitro-1*H*-pyrazole-3,5-dicarboxamide (3.00 g, 15.00 mmol) in acetonitrile (70 mL) at 0 °C was added $POCl_3$ (7.00 mL, 75.00 mmol). It was stirred with heating in a sealed stainless-steel tube at 120 °C for 12 h. The mixture was poured into water/ice and extracted with ethyl acetate (3 × 50 mL). The organic layer was dried over Na_2SO_4, filtered, and evaporated to give **2** as a yellow solid. Yield: 80%; T_m (onset) = 120 °C; ^{13}C NMR (75 MHz, d_6-DMSO): 138.8, 119.7, 111.7; IR (ν, cm^{-1}): 3186, 3148, 3013, 2877, 2833, 2740, 2589, 2266, 1699, 1582, 1546, 1473, 1449, 1361, 1296, 1192, 1141, 1050, 829, 797, 744, 665. Elemental analysis: Calcd (%) for $C_5HN_5O_2$ (163.09): C, 36.82; H, 0.62; N, 42.94; Found: C 37.08, H 0.92, N 42.50.

4.2.3. Synthesis of 5,5′-(1H-pyrazole-3,5-diyl)bis(1H-tetrazole) (3)

To a 100 mL round-bottomed flask was added **1** (0.70 g, 6.0 mmol), sodium azide (0.84 g, 13.0 mmol), zinc chloride (0.40 g, 3.0 mmol), and water (30 mL). The reaction mixture was stirred at reflux for 24 h. After cooling, HCl (3 M, 20 mL) was added to the reaction mixture with vigorous stirring. The reaction mixture was heated at 50 °C (until the white solid disappeared) and allowed to cool at room temperature. The crystalline compound was filtered and dried to give **3** as a white solid. Yield: 93%; T_d (onset) = 292 °C; ^{1}H NMR (300 MHz, d_6-DMSO): 7.4 (s, 1H); ^{13}C NMR (75 MHz, d_6-DMSO): 149.3, 134.8, 105.6; IR (ν, cm^{-1}): 3428, 3111, 2904, 2677, 1613, 1528, 1475, 1379, 1336, 1249, 1204, 1143, 1079, 1045, 968, 873, 834, 742, 534; Elemental analysis: Calcd (%) for $C_5H_4N_{10}$ (204.15): C 29.42, H 1.97, N, 68.61; Found: C 29.11, H 2.71, N 68.27.

4.2.4. Synthesis of 5,5′-(4-nitro-1H-pyrazole-3,5-diyl)bis(1H-tetrazole) (4)

To a 100 mL round-bottomed flask was added **1** (0.81 g, 5.0 mmol), sodium azide (0.71 g, 11.0 mmol), zinc chloride (0.34 g, 2.5 mmol), and water (30 mL). The reaction mixture was stirred under reflux for 24 h. After cooling, HCl (3 M, 20 mL) was added to the reaction mixture with vigorous stirring. The reaction mixture was heated to 50 °C (until the white solid disappeared) and allowed to cool at room temperature. The mixture was extracted with ethyl acetate (3 × 20 mL). The combined organic layers were dried over Na_2SO_4, filtered, and evaporated to give **4** as a yellow solid. Yield: 89%; T_d (onset) = 251 °C; ^{13}C NMR (75 MHz, d_6-DMSO): 147.8, 131.5 ; IR (ν, cm^{-1}): 3495, 3243, 2754, 2671, 1895, 1655, 1615, 1549, 1480, 1392, 1304, 1236, 1164, 1140, 1112, 1081, 1027, 1003, 976, 955, 878, 827, 773, 740, 712, 648; Elemental analysis: Calcd (%) for $C_5H_3N_{11}O_2$ (249.15): C, 24.10; H, 1.21; N, 61.84; Found: C, 24.19; H, 1.43; N, 61.27.

4.2.5. Synthesis of 5,5′-(4-bromo-1H-pyrazole-3,5-diyl)bis(1H-tetrazole) (13)

To a 100 mL round-bottomed flask was added **3** (0.5 g, 2.4 mmol), potassium bromide (0.57 g, 4.8 mmol), Oxone® (0.73, 4.8 mmol), and water (40 mL). The reaction mixture was stirred at room temperature for 3 hr. The resulting precipitate was filtered and washed with water (3 × 10 mL) to give **5** as a light-yellow solid. Yield: 88%; T_d (onset) = 286 °C; ^{13}C NMR (75 MHz, d_6-DMSO): 149.7, 135.1, 94.2; IR (ν, cm^{-1}): 3509, 3084, 2899, 1850, 1615, 1514, 1461, 1376, 1321, 1293, 1227, 1099, 1045, 954, 840, 749, 676, 601; Elemental analysis: Calcd (%) for $C_5H_3BrN_{10}$ (283.05): C, 21.22; H, 1.07; N, 49.49; Found: C, 21.41; H, 1.25; N, 49.65.

4.2.6. General procedure for the synthesis of energetic salts (5–17)

Aqueous ammonia, hydrazine hydrate, hydroxylamine or 3,6,7-triamino-7*H*-[1,2,4]triazolo[4,3-*b*][1,2,4]triazol-2-ium) (2.0 mmol) was added to a suspension of **3, 4 or 13** (1.0 mmol) in CH_3CN (50 mL). The reaction mixture was heated to 50 °C and stirred for 30 min. The precipitate was collected by filtration to give the product, which was purified further by washing with CH_3CN (3 × 10 mL).

5: Yield: 92%; T_d (onset) = 302 °C; ^1H NMR (300 MHz, d_6-DMSO): 8.50 (s, 8H), 6.89 (s, 1H); ^{13}C NMR (75 MHz, d_6-DMSO): 154.8, 140.1, 101.4; IR (ν, cm^{-1}): 3045, 1905, 1700, 1622, 1423, 1369, 1236, 1208, 1136, 1093, 1037, 979, 829, 756, 533; Elemental analysis: Calcd (%) for $C_5H_{10}N_{12}$ (238.21): C, 25.21; H, 4.23; N, 70.56; Found: C 26.03, H 3.71, N 68.94.

6: Yield: 90%; T_d (onset) = 307 °C; ^1H NMR (300 MHz, d_6-DMSO): 7.18 (s, 10*H*), 6.93 (s, 1H); ^{13}C NMR (75 MHz, d_6-DMSO): 154.8, 140.2, 101.2; IR (ν, cm^{-1}): 3316, 3136, 2922, 2631, 1628, 1519, 1395, 1369, 1339, 1247, 1180, 1131, 1037, 976, 960, 822, 755, 534; Elemental analysis: Calcd (%) for $C_5H_{12}N_{14}$ (268.24): C, 22.39; H, 4.51; N, 73.10; Found: C 22.49, H 4.53, N 70.47.

7: Yield: 94%; T_d (onset) = 307 °C; ^1H NMR (300 MHz, d_6-DMSO): 9.00 (s, 6H), 7.00 (s, 1H); ^{13}C NMR (75 MHz, d_6-DMSO): 153.1, 138.9, 101.5; IR (ν, cm^{-1}): 3027, 2727, 1617, 1547, 1479, 1404, 1375, 1350, 1245, 1206, 1182, 1138, 1046, 982, 824, 755, 536; Elemental analysis: Calcd (%) for $C_5H_{10}N_{12}O_2$ (270.21): C, 22.22; H, 3.73; N, 62.20; Found: C 22.25, H 3.76, N 61.33.

8: Yield: 85%; T_d (onset) = 248 °C; ^1H NMR (300 MHz, d_6-DMSO): 7.12 (s, 1H), 6.95 (s, 8H), 5.76 (s, 4H); ^{13}C NMR (75 MHz, d_6-DMSO): 159.6, 152.0, 148.2, 142.4, 138.0, 102.2; IR (ν, cm^{-1}): 3321, 3126, 2892, 1667, 1576, 1507, 1408, 1366, 1247, 1178, 1084, 1036, 974, 893, 841, 709, 604, 536; Elemental analysis: Calcd (%) for $C_{11}H_{16}N_{26}$ (512.42): C, 25.78; H, 3.15; N, 71.07; Found: C 26.19, H 3.03, N 71.09.

9: Yield: 93%; T_d (onset) = 278 °C; ^1H NMR (300 MHz, d_6-DMSO): 7.04 (s, 8H); ^{13}C NMR (75 MHz, d_6-DMSO): 151.8 1, 135.8 3, 130.1; IR (ν, cm^{-1}): 3175, 3058, 2885, 1871, 1700, 1612, 1565, 1519, 1452, 1389, 1359, 1310, 1268, 1194, 1137, 1081, 969, 827, 751, 711, 663; Elemental analysis: Calcd (%) for $C_5H_9N_{13}O_2$ (283.21); C, 21.20; H, 3.20; N, 64.29; Found: C 21.39, H 3.57, N 62.89. Calcd (%) for $C_5H_9N_{13}O_2{\cdot}0.5H_2O$ (292.22); C, 20.55; H, 3.45; N, 62.31; Found: C 20.78, H 3.24, N 61.37.

10: Yield: 92%; T_d (onset) = 212 °C; ^1H NMR (300 MHz, d_6-DMSO): 6.70 (s, 10*H*); ^{13}C NMR (75 MHz, d_6-DMSO): 152.0, 135.9, 129.9; IR (ν, cm^{-1}): 3023, 1609, 1507, 1387, 1356, 1315, 1195, 1105, 968, 829, 753, 703, 656; Elemental analysis: Calcd (%) for $C_5H_{11}N_{15}O_2$ (313.24): C, 19.17; H, 3.54; N, 67.07; Found: C 19.36, H 3.81, N 62.33.

11: Yield: 92%; T_d (onset) = 258 °C; ^1H NMR (300 MHz, d_6-DMSO): 8.66 (s, 6H); ^{13}C NMR (75 MHz, d_6-DMSO): 152.2, 151.7, 135.6; IR (ν, cm^{-1}): 3145, 3036, 2736, 1612, 1519, 1453, 1386, 1207, 1140, 1062, 1002, 965, 829, 751, 700; Elemental analysis: Calcd (%) for $C_5H_9N_{13}O_4$ (315.21): C, 19.05; H, 2.88; N, 57.77; Found: C 18.98, H 2.74, N 57.56.

12: Yield: 84%; T_d (onset) = 260 °C; ^1H NMR (300 MHz, d_6-DMSO): 7.64 (s, 2H), 7.07 (s, 2H), 6.71 (s, 2H), 5.76 (s, 2H); ^{13}C NMR (75 MHz, d_6-DMSO): 159.8, 150.8, 147.8, 141.8, 135.0, 130.0; IR (ν, cm^{-1}): 3387, 3235, 3127, 2917, 2740, 1659, 1510, 1389, 1345, 1163, 1040, 963, 837, 715, 623; Elemental analysis: Calcd (%) for $C_{11}H_{15}N_{27}O_2$ (557.42): C, 23.70; H, 2.71; N, 67.85; Found: C 23.23, H 3.02, N 65.87.

14: Yield: 94%; T_d (onset) = 286 °C; ^1H NMR (300 MHz, d_6-DMSO): 8.16 (s, 8H); ^{13}C NMR (75 MHz, d_6-DMSO): 153.3, 138.8, 90.5; IR (ν, cm^{-1}): 3285, 3171, 3050, 2843, 2172, 1883, 1680, 1434, 1356, 1322, 1199, 1166, 1065, 995, 960, 707, 601; Elemental analysis: Calcd (%) for $C_5H_9BrN_{12}$ (317.11): C, 18.94; H, 2.86; N, 53.00; Found: C 19.05, H 2.89, N 52.41.

15: Yield: 93%; T_d (onset) = 212 °C; ^1H NMR (300 MHz, d_6-DMSO): 7.63 (s, 10*H*); ^{13}C NMR (75 MHz, d_6-DMSO): 153.4, 139.0, 90.3; IR (ν, cm^{-1}): 3321, 3227, 3127, 3045, 2909, 2725, 2635, 1608, 1534, 1495, 1398, 1356, 1319, 1254, 1108, 963, 801, 600; Elemental analysis: Calcd (%) for $C_5H_{11}BrN_{14}$ (347.14): C, 17.30; H, 3.19; N, 56.49; Found: C 17.33, H 3.16, N 55.60.

16: Yield: 95%; T_d (onset) = 252 °C; ^1H NMR (300 MHz, d_6-DMSO): 8.51 (s, 6H); ^{13}C NMR (75 MHz, d_6-DMSO): 152.9, 138.6, 90.4; IR (ν, cm^{-1}): 3145, 3046, 2908, 2734, 1616, 1435, 1356, 1323, 1204, 1131, 995, 962, 816, 759, 706, 602; Elemental analysis: Calcd (%) for $C_5H_9BrN_{12}O_2$ (349.11): C, 17.20; H, 2.60; N, 48.15; Found: C 17.65, H 2.99, N 49.46.

17: Yield: 90%; T_d (onset) = 255 °C; ^1H NMR (300 MHz, d_6-DMSO): 6.83 (s, 4H), 5.70 (s, 2H); ^{13}C NMR (75 MHz, d_6-DMSO): 159.4, 151.1, 148.2, 142.3, 137.3; IR (ν, cm^{-1}): 3277, 3178, 3087, 1683, 1508, 1444, 1415, 1354, 1323, 1165, 1111, 1029, 951, 838, 721, 596; Elemental analysis: Calcd (%) for $C_{11}H_{15}BrN_{26}$ (591.32): C, 22.34; H, 2.56; N, 61.59; Found: C 22.35, H 2.68, N 61.25.

4.2.7. Synthesis of 5,5′-(4-chloro-1H-pyrazole-3,5-diyl)bis(1H-tetrazole) (18)

To a 100 mL round-bottomed flask was added **3** (0.50 g, 2.40 mmol), potassium chloride (0.36 g, 4.80 mmol), Oxone® (0.73, 4.8 mmol), and water (40 mL). The reaction mixture was stirred at room temperature for 3 hr. The resulting precipitate was filtered and washed with water (3 × 50 mL) to give **5** as a light-yellow solid. Yield: 83%; T_d (onset) = 276 °C; ^{13}C NMR (75 MHz, d_6-DMSO): 149.2, 132.4, 109.0; IR (ν, cm^{-1}): 3436, 3162, 3076, 2909, 2749, 2679, 2140, 1618, 1506, 1477, 1334, 1265, 1174, 1039, 952, 612; Elemental analysis: Calcd (%) for $C_5H_3ClN_{10}$ (238.60): C, 25.17; H, 1.27; N, 58.70; Found: C, 25.22; H, 1.61; N, 57.63.

4.2.8. Synthesis of 5,5′-(4-iodo-1H-pyrazole-3,5-diyl)bis(1H-tetrazole) (19)

To a 100 mL round-bottomed flask was added **3** (0.50 g, 2.40 mmol), potassium iodide (0.79 g, 4.80 mmol), Oxone® (0.73, 4.8 mmol), and water (40 mL). The reaction mixture was stirred at room temperature for 3 hr. The resulting precipitate is filtered and washed with water to give **5** and **3** as an inseparable mixture. ^{13}C NMR (75 MHz, d_6-DMSO): 150.6 (*C*HN_4), 139.4 (*C*3,*C5*), 61.9 (*C4* − I).

4.2.9. Synthesis of 5,5′-(1H-pyrazole-3,5-diyl)bis(1H-tetrazol-1-ol) (20)

To a 100 mL round-bottomed flask was added **3** (0.50 g, 2.40 mmol) and NaOH (2 eq) in water (40 mL). Oxone® (0.73, 4.8 mmol) was added to the reaction mixture and stirred at 40 °C for 12 hrs. Concentrated HCl was added dropwise to the reaction mixture at room temperature until the product precipitated. The resulting precipitate was filtered and washed with water (3 × 50 mL) to give **20** as a white solid. Yield: 70%; T_d (onset) = 270 °C; ^{1}H NMR (300 MHz, d_6-DMSO): 7.50 (s, 1H); ^{13}C NMR (75 MHz, d_6-DMSO): 149.23, 132.1, 109.1; IR (ν, cm^{-1}): 3524, 3162, 3068, 2842, 2668, 1870, 1621, 1511, 1381, 1307, 1220, 1098, 1037, 950, 827, 749, 613; Elemental analysis: Calcd (%) for $C_5H_4N_{10}O_2$ (236.15): C, 25.43; H, 1.71; N, 59.31; Found: C, 25.03; H, 1.67; N, 58.14.

21: Yield: 92%; T_d (onset) = 291 °C; ^{1}H NMR (300 MHz, d_6-DMSO): 8.03 (s, 8H), 6.95 (s, 1H); ^{13}C NMR (75 MHz, d_6-DMSO): 153.0, 137.2, 104.9; IR (ν, cm^{-1}): 3289, 3170, 3051, 2851, 1885, 1678, 1613, 1438, 1361, 1168, 1132, 1066, 1002, 963, 763, 612; Elemental analysis: Calcd (%) for $C_5H_{10}N_{12}O_2$ (270.21): C, 22.22; H, 3.73; N, 62.20; Found: C 22.63, H 3.72, N 61.25.

22: Yield: 90%; T_d (onset) = 296 °C; ^{1}H NMR (300 MHz, d_6-DMSO): 9.28 (s, 10*H*), 7.73 (s, 1H); ^{13}C NMR (75 MHz, d_6-DMSO): 153.1, 137.2, 104.9; IR (ν, cm^{-1}): 3329, 3219, 3132, 2912, 2733, 2626, 1609, 1532, 1486, 1398, 1357, 1323, 1258, 1105, 961, 814, 690; Elemental analysis: Calcd (%) for $C_5H_{12}N_{14}O_2$ (300.24) C, 20.00; H, 4.03; N, 65.31; Found: C 20.08, H 3.74, N 64.84.

Declaration of Competing Interest

The authors declare that they have no known competing financial interests or personal relationships that could have appeared to influence the work reported in this paper.

Acknowledgement

The Rigaku Synergy S Diffractometer was purchased with support from the MRI program of the National Science Foundation (Grant no. 1919565).

Appendix A. Supplementary data

Supplementary data to this article can be found online at https://doi.org/10.1016/j.cej.2021.133282.

References

[1] J.P. Agrawal, *High Energy Materials*, Wiley, 2010. https://doi.org/10.1002/9783527628803. (b) T. M. Klapötke, *High Energy Density Materials*, Springer: Berlin, 2007. https://doi.org/10.1007/978-3-540-72202-1.
[2] H. Gao, J.M. Shreeve, Azole-based energetic salts, Chem. Rev. 111 (2011) 7377–7436, https://doi.org/10.1021/cr200039c.
[3] (a) H. Wei, C. He, J. Zhang, J.M. Shreeve, Combination of 1,2,4-oxadiazole and 1,2,5-oxadiazole moieties for the generation of high-performance energetic materials, Angew. Chem., Int. Ed. 54 (2015) 9367–9371, https://doi.org/10.1002/anie.201503532;
(b) P. Yin, J. Zhang, G.H. Imler, D.A. Parrish, J.M. Shreeve, Polynitro-functionalized dipyrazolo-1,3,5-triazinanes: energetic polycyclization toward high density and excellent molecular stability, Angew. Chem., Int. Ed. 56 (2017) 8834–8838, https://doi.org/10.1002/anie.201704687;
(c) J. Zhang, P. Yin, L.A. Mitchell, D.A. Parrish, J.M. Shreeve, N-functionalized nitroxy/azido fused-ring azoles as high-performance energetic materials, J. Mater. Chem. A. 4 (2016) 7430–7436, https://doi.org/10.1039/C6TA02384C.
[4] G. da Silva, J.W. Bozzelli, Retro-[3 + 2]-cycloaddition reactions in the decomposition of five-membered nitrogen-containing heterocycles, J. Org. Chem. 73 (2008) 1343–1353, https://doi.org/10.1021/jo701914y.
[5] (a) M. Göbel, K. Karaghiosoff, T.M. Klapötke, D.G. Piercey, J. Stierstorfer, Nitrotetrazolate-2 N -oxides and the strategy of n -oxide introduction, J. Am. Chem. Soc. 132 (2010) 17216–17226, https://doi.org/10.1021/ja106892a;
(b) T.M. Klapötke, C.M. Sabaté, J. Stierstorfer, Neutral 5-nitrotetrazoles: easy initiation with low pollution, New J. Chem. 33 (2009) 136–147, https://doi.org/10.1039/B812529E.
[6] F.R. Benson, The chemistry of the tetrazoles, Chem. Rev. 41 (1947) 1–61, https://doi.org/10.1021/cr60128a001.
[7] (a) D. Kumar, G.H. Imler, D.A. Parrish, J.M. Shreeve, Aminoacetonitrile as precursor for nitrogen rich stable and insensitive asymmetric N-methylene-C linked tetrazole-based energetic compounds, J. Mater. Chem. A. 5 (2017) 16767–16775, https://doi.org/10.1039/C7TA05394K;
(b) T. Wang, H. Gao, J.M. Shreeve, Functionalized tetrazole energetics: a route to enhanced performance, zeitschrift für anorg. und Allg, Chemie. 647 (2021) 157–191, https://doi.org/10.1002/zaac.202000361;
(c) M.H.H. Wurzenberger, S.M.J. Endraß, M. Lommel, T.M. Klapötke, J. Stierstorfer, Comparison of 1-propyl-5 h -tetrazole and 1-azidopropyl-5 h -tetrazole as ligands for laser ignitable energetic materials, ACS Appl. Energy Mater. 3 (2020) 3798–3806, https://doi.org/10.1021/acsaem.0c00229.
[8] (a) P. Pagoria, A comparison of the structure, synthesis, and properties of insensitive energetic compounds, propellants, Explos. Pyrotech. 41 (2016) 452–469, https://doi.org/10.1002/prep.201600032;
(b) M.H. Keshavarz, H. Soury, H. Motamedoshariati, A. Dashtizadeh, Improved method for prediction of density of energetic compounds using their molecular structure, Struct. Chem. 26 (2015) 455–466, https://doi.org/10.1007/s11224-014-0502-7.
[9] H. Li, L. Zhang, N. Petrutik, K. Wang, Q. Ma, D. Shem-Tov, F. Zhao, M. Gozin, Molecular and crystal features of thermostable energetic materials: guidelines for architecture of "bridged" compounds, ACS Cent. Sci. 6 (2020) 54–75, https://doi.org/10.1021/acscentsci.9b01096.
[10] (a) D. Kumar, G.H. Imler, D.A. Parrish, J.M. Shreeve, Resolving synthetic challenges faced in the syntheses of asymmetric N, N′-ethylene-bridged energetic compounds, New J. Chem. 41 (2017) 4040–4047, https://doi.org/10.1039/C7NJ00327G;
(b) Y. Tang, H. Gao, D.A. Parrish, J.M. Shreeve, 1,2,4-triazole links and n -azo bridges yield energetic compounds, Chem. - A Eur. J. 21 (2015) 11401–11407;
(c) A.K. Chinnam, Q. Yu, G.H. Imler, D.A. Parrish, J.M. Shreeve, Azo- and methylene-bridged mixed azoles for stable and insensitive energetic applications, Dalt. Trans. 49 (2020) 11498–11503, https://doi.org/10.1039/D0DT02223C;
(d) L. Türker, Azo-bridged triazoles: Green energetic materials, Def. Technol. 12 (2016) 1–15, https://doi.org/10.1016/j.dt.2015.11.002.
[11] A.K. Ma, G. Chinnam, H. Cheng, J. Yang, J.M.S. Zhang, 1,3,4-Oxadiazole Bridges: A strategy to improve energetics at the molecular level, Angew. Chem., Int. Ed. 60 (2021) 5497–5504, https://doi.org/10.1002/anie.202014207.
[12] T. Yan, G. Cheng, H. Yang, 1,2,4-oxadiazole-bridged polynitropyrazole energetic materials with enhanced thermal stability and low sensitivity, Chempluschem. 84 (2019) 1567–1577, https://doi.org/10.1002/cplu.201900454.
[13] (a) M. Faisal, A. Saeed, S. Hussain, P. Dar, F.A. Larik, Recent developments in synthetic chemistry and biological activities of pyrazole derivatives, J. Chem. Sci. 131 (2019) 70. https://doi.org/10.1007/s12039-019-1646-1. (b) A.W. Brown, Recent Developments in the Chemistry of Pyrazoles, in: Adv. Heterocycl. Chem., 2018: pp. 55–107. https://doi.org/10.1016/bs.aihch.2018.02.001.
[14] Ş.G. Küçükgüzel, S. Şenkardeş, Recent advances in bioactive pyrazoles, Eur. J. Med. Chem. 97 (2015) 786–815, https://doi.org/10.1016/j.ejmech.2014.11.059.
[15] (a) C. Lei, H. Yang, G. Cheng, New pyrazole energetic materials and their energetic salts: combining the dinitromethyl group with nitropyrazole, Dalt. Trans. 49 (2020) 1660–1667, https://doi.org/10.1039/C9DT04235K;
(b) C. Lei, G. Cheng, Z. Yi, Q. Zhang, H. Yang, A facile strategy for synthesizing promising pyrazole-fused energetic compounds, Chem. Eng. J. 416 (2021), 129190, https://doi.org/10.1016/j.cej.2021.129190.
[16] M.A. Spackman, J.J. McKinnon, Fingerprinting intermolecular interactions in molecular crystals, CrystEngComm. 4 (2002) 378–392, https://doi.org/10.1039/B203191B.
[17] M.A. Spackman, D. Jayatilaka, Hirshfeld surface analysis, CrystEngComm. 11 (2009) 19–32, https://doi.org/10.1039/B818330A.
[18] E.R. Johnson, S. Keinan, P. Mori-Sánchez, J. Contreras-García, A.J. Cohen, W. Yang, Revealing noncovalent interactions, J. Am. Chem. Soc. 132 (2010) 6498–6506, https://doi.org/10.1021/ja100936w.
[19] R. Mayer, J. Köhler and A. Homburg, *Explosives*, Wiley VCH, Weinheim, 6th edn, 2007.
[20] Y. Tang, C. He, L.A. Mitchell, D.A. Parrish, J.M. Shreeve, C-N bonded energetic biheterocyclic compounds with good detonation performance and high thermal stability, J. Mater. Chem. A. 4 (2016) 3879–3885, https://doi.org/10.1039/C5TA09803C.
[21] M. Zhang, P.F. Pagoria, G.H. Imler, D. Parrish, Trimerization of 4-Amino-3,5-dinitropyrazole: formation, preparation, and characterization of 4-Diazo-3,5-bis(4-amino-3,5-dinitropyrazol-1-yl) pyrazole (LLM-226), J. Heterocycl. Chem. 56 (2019) 781–787, https://doi.org/10.1002/jhet.3434.
[22] Y. Wang, Y. Liu, S. Song, Z. Yang, X. Qi, K. Wang, Y. Liu, Q. Zhang, Y. Tian, Accelerating the discovery of insensitive high-energy-density materials by a materials genome approach, Nat. Commun. 9 (2018) 2444, https://doi.org/10.1038/s41467-018-04897-z.
[23] Bruker, *APEX2 v2010.3-0*, Bruker AXS Inc., Madison, Wisconsin, USA, 2014.
[24] Bruker, *SAINT v7.68A*, Bruker AXS Inc., Madison, Wisconsin, USA, 2009.
[25] Bruker, *XPREP v2008/2*, Bruker AXS Inc., Madison, Wisconsin, USA, 2014.
[26] .R. and W. Yang, Density Functional Theory of Atoms and Molecules. Oxford University Press: New York, Density Funct. Theory Atoms Mol. (1989).

[27] O.M. Suleimenov, T.-K. Ha, Ab initio calculation of the thermochemical properties of polysulphanes (H2Sn), Chem. Phys. Lett. 290 (1998) 451–457, https://doi.org/10.1016/S0009-2614(98)00512-0.
[28] H.D.B. Jenkins, D. Tudela, L. Glasser, Lattice potential energy estimation for complex ionic salts from density measurements, Inorg. Chem. 41 (2002) 2364–2367, https://doi.org/10.1021/ic011216k.
[29] M.S. Westwell, M.S. Searle, D.J. Wales, D.H. Williams, Empirical correlations between thermodynamic properties and intermolecular forces, J. Am. Chem. Soc. 117 (1995) 5013–5015, https://doi.org/10.1021/ja00123a001.